

# Characterization of Functionalized Single-Walled Carbon Nanotubes at Individual Nanotube-Thin Bundle Level

Yi Lin,<sup>†</sup> Darron E. Hill,<sup>†</sup> James Bentley,<sup>‡</sup> Lawrence F. Allard,<sup>\*,§</sup> and Ya-Ping Sun<sup>\*,†</sup>

Department of Chemistry and Center for Advanced Engineering Fibers and Films, Howard L. Hunter Chemistry Laboratory, Clemson University, Clemson, South Carolina 29634-0973, Metals and Ceramics Division and High Temperature Materials Laboratory, Oak Ridge National Laboratory, Oak Ridge, Tennessee 37831-6062

Received: May 12, 2003; In Final Form: June 23, 2003

Individual and thin bundles of aminopolymer-functionalized single-walled carbon nanotubes (SWNTs) were successfully imaged using high-resolution transmission electron microscopy (HR-TEM). The corresponding electron energy loss spectroscopy (EELS) characterization of the same TEM specimen before and after ex situ thermal defunctionalization confirmed that the nanotube surface was covered with nitrogen-containing functionalities in the functionalized SWNT sample.

## Introduction

Functionalization of single-walled carbon nanotubes (SWNTs) with various inorganic and organic substances has become a significant topic recently.<sup>1–3</sup> The surfaces of SWNTs have been modified, and sometimes passivated, to achieve solubilization in organic solvents and/or water using approaches that involve either covalent linkages (such as defect-targeted<sup>1,2,4–8</sup> or side-wall-targeted<sup>3</sup>) or noncovalent interactions (such as polymer-wrapping<sup>9</sup> or  $\pi$ – $\pi$  stacking<sup>10</sup>). Methods for the characterization of these functionalized SWNTs usually include solution-based spectroscopic techniques, such as UV–vis, near-IR, and NMR, and solid phase techniques, such as thermal gravimetric analysis (TGA) and Raman spectroscopy. In addition, microscopy and related tools provide valuable visual information on the structure of functionalized carbon nanotubes. For example, atomic force microscopy (AFM) has been widely used to study the aggregation status of functionalized SWNTs and functional group–nanotube interactions. Scanning tunneling microscopy (STM) has provided atomic-level characterization of polymer-functionalized SWNTs.<sup>11</sup> Scanning electron microscopy (SEM) has been especially useful for defunctionalized specimens, because strong surface charging effects are suppressed after partial removal of nonconductive functional groups.<sup>2</sup>

Transmission electron microscopy (TEM) is one of the most widely used microscopy techniques for characterizing carbon nanotubes because it provides not only global information on nanotube purity and dispersity but also subnanometer information at high-magnification. Even atomic-resolution images of SWNTs can be obtained when optimized.<sup>12</sup> When TEM is coupled with other analysis tools, such as energy-dispersive X-ray spectroscopy (EDX) or electron energy loss spectroscopy (EELS), detailed information can be obtained on the elemental components of various derivatized carbon nanotubes. For example, Golberg and co-workers reported high-resolution TEM (HR-TEM) and EELS characterization of B-doped and N-doped SWNT bundles.<sup>13</sup> Suenaga and co-workers successfully identi-

fied and mapped a chain of metallofullerene molecules ( $\text{Gd}@\text{C}_{82}$ ) inside a SWNT through element-selective single atom imaging based on EELS.<sup>14</sup> More recently, Hayashi and co-workers noted two significant findings during EELS studies of “nanoTeflons” from fluorinated multiple-walled carbon nanotubes (MWNTs).<sup>15</sup> They found that both ionic and covalent bonding exist between C and F atoms. In addition, they found that atomic fluorine covers not only the full length of the outer layer but also the inner layer of MWNTs.<sup>15</sup>

Despite the wealth of information revealed by the techniques discussed above, questions remain about the fundamental properties of the functionalized SWNTs. These could be answered through direct HR-TEM imaging and corresponding analysis of the functionalized SWNTs at the individual nanotube–thin bundle level, including bundling–debundling structure and the location of functional groups. We report here such imaging and analysis of individual and thin bundles of aminopolymer-functionalized SWNTs, with related EELS characterization. The specimens were subjected to ex situ thermal defunctionalization on specially designed TEM grids. Results obtained before and after the thermal defunctionalization are also compared and discussed.

## Experimental Section

**Materials.** Poly(propionylethylenimine) (PPEI,  $M_w \sim 200\,000$ ) was purchased from Aldrich and hydrolyzed into poly(propionylethylenimine-co-ethylenimine) (PPEI-EI, the mole fraction of EI  $\sim 15\%$ ) as reported previously.<sup>16</sup> [1-Ethyl-3-(dimethylamino)propyl]carbodiimide hydrochloride (EDAC) was obtained from Alfa Aesar. Dialysis membrane tubings were supplied by Spectrum Laboratories. Holey carbon-coated copper and stainless steel grids were obtained from Structure Probe, Inc. Holey  $\text{LaCrO}_3$ -coated grids were prepared by sputtering a thin layer of  $\text{LaCrO}_3$  (ca. 15 nm) on holey carbon-coated stainless steel grids, followed by thermal removal of the carbon layer.

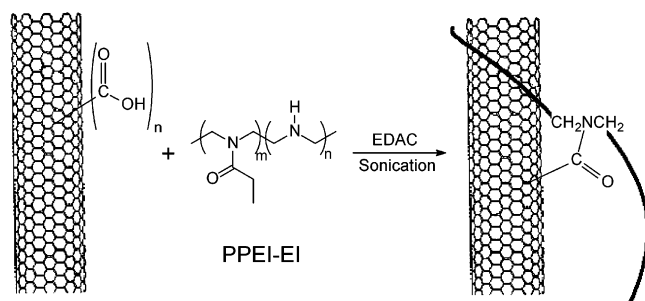
The SWNT sample was produced using the arc-discharge method in Professor A. M. Rao’s laboratory in the Department of Physics and Astronomy at Clemson University. In the purification, an as-produced SWNT sample (1 g) was suspended in nitric acid (2.6 M, 200 mL) and the suspension was refluxed

<sup>†</sup> Clemson University.

<sup>‡</sup> Metals and Ceramics Division, Oak Ridge National Laboratory.

<sup>§</sup> High Temperature Materials Laboratory, Oak Ridge National Laboratory.

## SCHEME 1



for 48 h. After the suspension was vigorously centrifuged and the supernatant was discarded, the remaining solids were washed repeatedly with deionized water and dried under vacuum.

**Measurements.** HR-TEM analyses were conducted on a 200 kV Hitachi HF-2000 analytical electron microscope equipped with a field emission gun and a Gatan 794 Multi-Scan CCD camera for digital imaging. EELS spectra and the corresponding TEM images were obtained on a 300 kV Philips CM30 TEM-STEM system at a collection angle of 4.8 mrad and convergence angle of 1 mrad. Because the electron beam can damage SWNTs, and more so the functional groups on the SWNT surface, the HR-TEM imaging was performed rapidly (typically 1–2 min).

**Functionalization of SWNTs with PPEI-EI.** The functionalization was based on the carbodiimide-activated amidation reaction (Scheme 1). In a typical experiment, a purified SWNT sample (19.7 mg) and EDAC (160 mg) were added to an aqueous  $\text{KH}_2\text{PO}_4$  buffer solution (15 mL) and the mixture was sonicated for 30 min under  $\text{N}_2$  protection. PPEI-EI (198 mg) in the same buffer (5 mL) was added to the above solution via a syringe. The mixture was further sonicated for 24 or 48 h under  $\text{N}_2$  protection, followed by centrifuging at 7800 rpm to separate the insoluble residue. The soluble fraction was then placed into a dialysis tubing (cutoff molecular weight 2000) and dialyzed against freshwater for 3 days. The dark aqueous solution thus obtained was used to prepare specimens for TEM and EELS characterizations.

## Results and Discussion

SWNTs, after oxidative acid treatment during purification, contain carboxylic acid moieties of ca. 2 mol % at open ends and defect sites on the sidewalls.<sup>17</sup> These carboxylic acids have been used in the defect-targeted functionalization and solubilization of carbon nanotubes with amine- or hydroxy-containing functional groups.<sup>1,2</sup> A carbodiimide-activated amidation reaction was used in the present work to prepare soluble PPEI-EI-functionalized SWNTs (Scheme 1). In the reaction, the acid was converted into *N*-hydroxysuccinimide by EDAC with the aid of continuous sonication, followed by the coupling with the secondary amine groups of the PPEI-EI to form amide linkages. We have reported previously that prolonged sonication in the carbodiimide-activated functionalization of MWNTs with PPEI-EI could shorten the nanotubes and increase the nanotube uptake into solution.<sup>16</sup> For SWNTs, Figure 1 shows that after sonication reaction for 48 h, most of the nanotubes are less than 500 nm in length, which are shorter than those in the starting material before reaction. All functionalized SWNT samples in this study were obtained from the reactions with sonication for 24 or 48 h.

Commercially available holey carbon-coated grids were used in the TEM analysis of our functionalized SWNT samples.

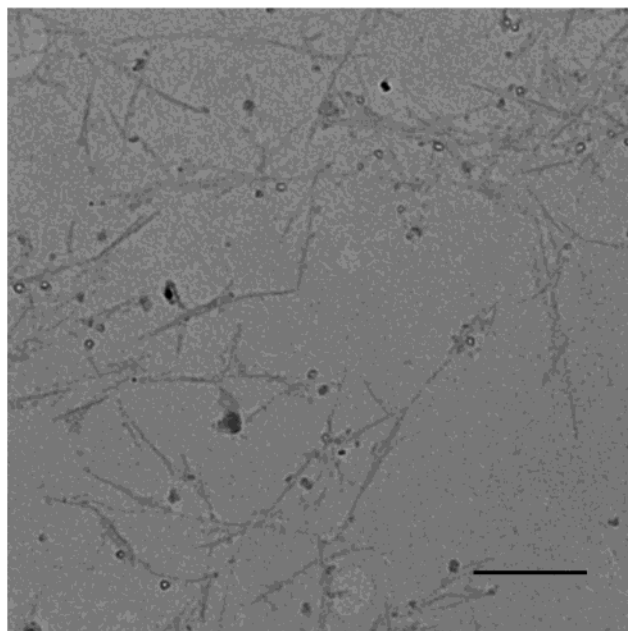


**Figure 1.** TEM image of PPEI-EI-functionalized SWNTs prepared via carbodiimide-activated reaction with sonication for 48 h (scale bar = 500 nm).

Generally, the nanotubes must be across a hole to provide enough image contrast to resolve the nanotube wall structure and observe the substance on or in an individual SWNT or a thin bundle of SWNTs. In a typical experiment, a TEM specimen was prepared by using an inoculating loop to place several drops of a dark aqueous solution of PPEI-EI-functionalized SWNTs onto a holey carbon-coated grid. These functionalized SWNTs, especially the longer ones ( $>1\ \mu\text{m}$ ), apparently have a tendency to cluster around the hole edges rather than to extend across the holes, as seen in Figure 2. The high aspect ratios of SWNTs combined with exfoliation of the bundles during the functionalization reaction are likely to be the major reasons for such an “edge effect”.<sup>18</sup> Furthermore, because SWNTs are functionalized with hydrophilic aminopolymers, the nanotube surfaces are “wetted” by the polymers, as discussed below. Therefore, during the solvent evaporation, the surface tension might be in favor of dragging the nanotubes to the edge of the holes. The “edge effect” is more pronounced in a sample containing longer nanotubes obtained with less sonication time in the functionalization reaction. Nevertheless, the abundance of PPEI-EI-functionalized SWNTs in the specimen did result in some SWNTs extending across the holes, making it possible to distinguish between the nanotubes and the thin amorphous carbon bridges of the holey carbon-coated grid itself.

Functionalization is known to exfoliate the bundles of SWNTs into isolated nanotubes and thinner bundles. Figure 3 shows the first HR-TEM image of an individual polymer-functionalized SWNT.<sup>19</sup> This functionalized SWNT is  $\sim 1.5\ \text{nm}$  in diameter and  $\sim 70\ \text{nm}$  in observable length ( $\sim 40\ \text{nm}$  shown). Clearly, the nanotube surface is covered by a significant amount of polymers. Separately, a thin bundle of PPEI-EI-functionalized SWNTs is shown in Figure 4. The image also indicates the presence of polymers on the nanotube surfaces. These results allowed a direct examination of the PPEI-EI-functionalized carbon nanotube sample at the level of individual SWNTs or their thin bundles. In addition, we went to considerable effort to confirm that the materials on the nanotube surface were indeed associated primarily with the aminopolymer.



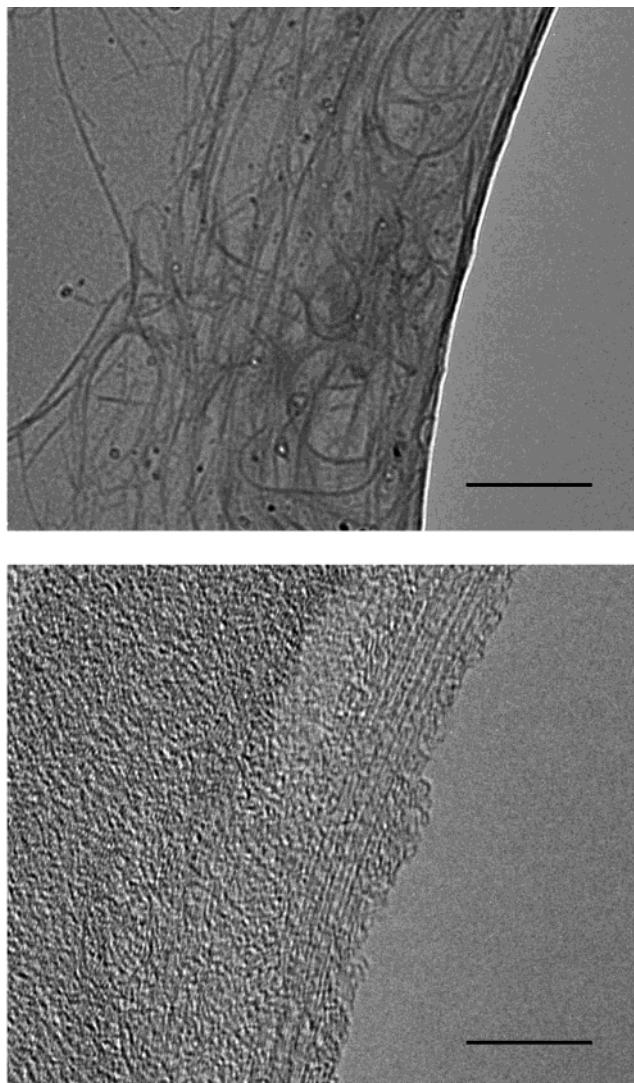


**Figure 2.** Typical TEM images at low (top, scale bar = 200 nm) and high (bottom, scale bar = 10 nm) magnification, illustrating the “edge effect” for the PPEI-EI-functionalized SWNTs on a holey-carbon grid.

For the aminopolymer PPEI-EI with EI mole fraction of 15% used in this study, nitrogen/carbon atomic ratio (N/C ratio) is calculated to be  $\sim 0.22$ . Therefore, nitrogen atoms in the aminopolymers could be conveniently used to probe the presence of the polymers themselves. EDX characterization was not successful because of overwhelming signals from C atoms that are so close to those from N atoms as to be unresolvable.

As discussed previously, EELS has been widely applied to characterize pristine and doped carbon nanotubes. The K-edges of C and N in the EELS spectra are 284 and 401 eV, respectively. This allows good resolution between C and N signals regardless of the broad feature of C-K EELS core loss.<sup>20</sup> Figure 5 shows a typical EELS spectrum for a thin bundle of PPEI-EI-functionalized SWNTs. From this spectrum, it was estimated that the N/C ratio in the view area (inset) was  $\sim 0.08$ . The EELS results for other areas selected randomly are similar, with all N/C values in the 0.07–0.1 range. Therefore, considering the significant C signals contributed by the SWNTs themselves, there is no doubt that the SWNTs are indeed attached primarily by the aminopolymer for functionalization.

EELS line scans were carried out in a cross-sectional direction through a thin bundle ( $\sim 30$  nm in diameter) of functionalized SWNTs. As shown in Figure 6, C and N concentration profiles correlate well, indicating a random distribution of polymers on

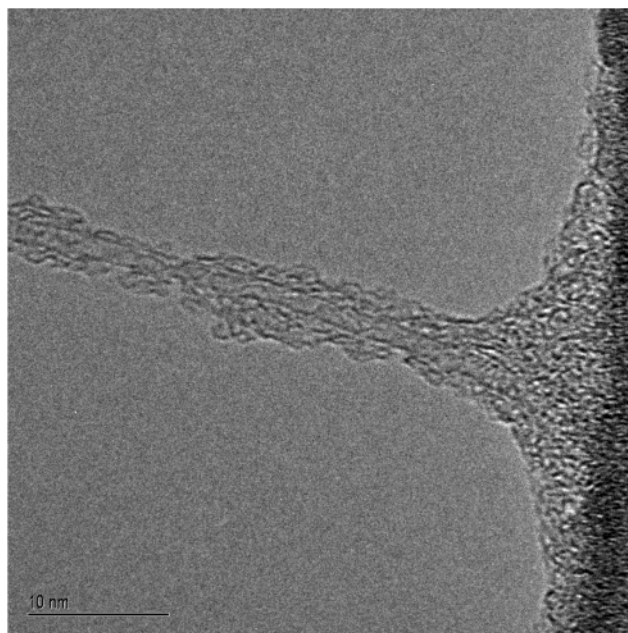


**Figure 3.** HR-TEM image of an individual PPEI-EI-functionalized SWNT (scale bar = 10 nm).

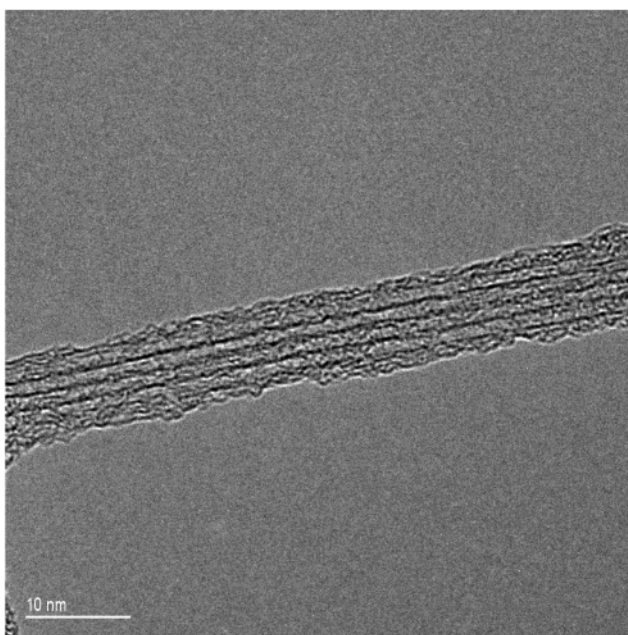


**Figure 4.** HR-TEM image of a PPEI-EI-functionalized SWNT bundle (scale bar = 10 nm).

the SWNTs with a relatively constant N/C ratio. Results from EELS elemental mapping over a relatively large area of functionalized SWNT also indicate that the N atoms (with the aminopolymer) are randomly distributed throughout the imaged material, agreeing well with the C-map.

Polymer-functionalized carbon nanotubes can be defunctionalized under elevated temperatures in either oxidative or inert atmosphere.<sup>2</sup> In particular, the PPEI-EI polymers are readily evaporated in the presence of air at a threshold temperature of  $\sim 340$  °C, at which SWNTs are relatively stable. Therefore, we have thermally defunctionalized the PPEI-EI-functionalized SWNTs for further characterization. To keep the SWNTs well dispersed, the thermal reactions were carried out ex situ for the specimens on the TEM grids. Because commonly used holey carbon-coated copper grids suffer from film decomposition and

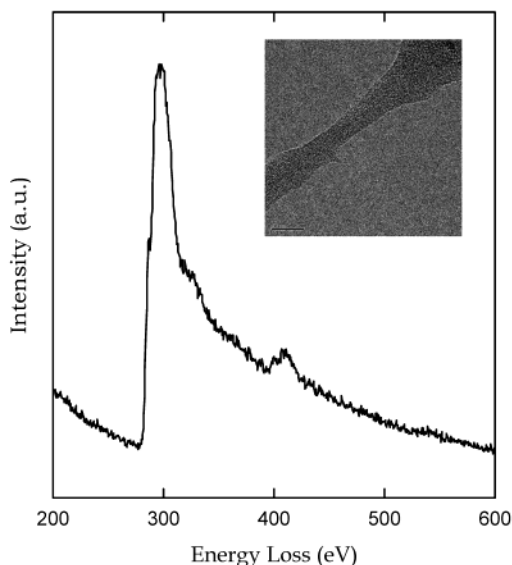


**Figure 5.** Typical EELS spectrum of a thin bundle of PPEI-EI-functionalized SWNTs, with the corresponding TEM image shown in the inset (scale bar = 20 nm).

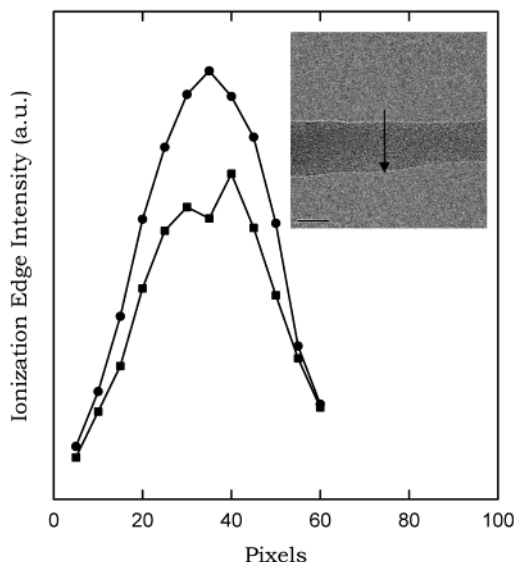


**Figure 6.** Concentration profiles of C (●) and N (■) of a thin bundle of PPEI-EI-functionalized SWNTs generated from EELS line scans in the arrow direction (inset, scale bar = 20 nm). The width of the bundle was divided into 60 pixels horizontally; thus, 12 EELS spectra were obtained by moving the probe 5 pixels vertically in each scan.

physical distortion of the grid structure at temperatures close to 400 °C, specially designed holey  $\text{LaCrO}_3$ -coated stainless steel grids were used. To achieve a partial removal of the polymers, the defunctionalization reactions were conducted at 370 °C for 10–20 min. Shown in Figure 7 is a typical HR-TEM image of a PPEI-EI-functionalized SWNT specimen after the thermal treatment. Compared to Figure 4, the SWNTs are much cleaner, with little material on the nanotube surface. Figure 8 shows that individual or thin bundles of SWNTs could easily be located on the TEM grids, with little or no polymers attached to the nanotubes.

Results from the EELS investigation are consistent with a successful thermal defunctionalization. As shown in Figure 9, the signal from N atoms at  $\sim 405$  eV is significantly lower in comparison with that in Figure 5, corresponding to a much reduced N/C ratio of  $\sim 0.02$ . This results from the fact that most

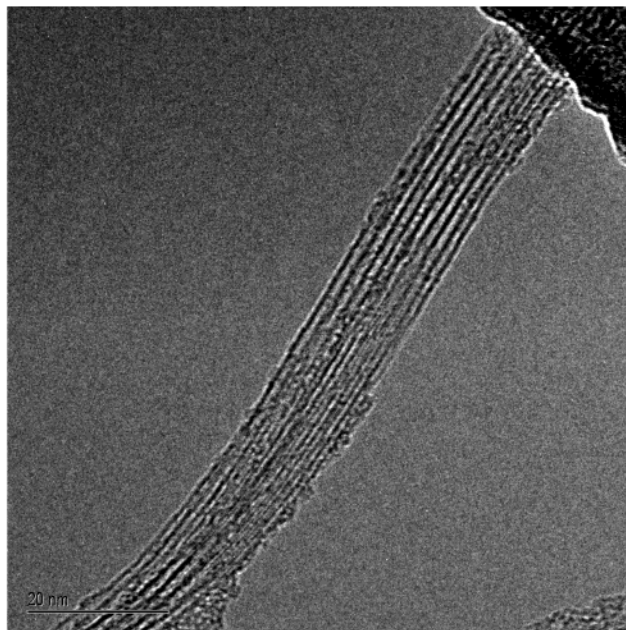


**Figure 7.** HR-TEM image of a thin bundle of PPEI-EI-functionalized SWNTs after ex situ thermal treatment (scale bar = 20 nm).

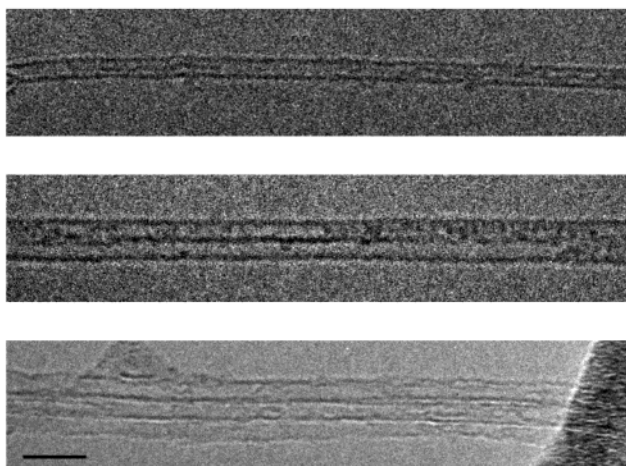


**Figure 8.** HR-TEM images of PPEI-EI-functionalized SWNTs after ex situ thermal treatment (scale bar = 10 nm).

of the nitrogen-containing polymers originally attached to the SWNTs are removed in the thermal defunctionalization process.

TEM imaging of functionalized SWNTs with various functional groups is intrinsically difficult, especially when there is ready dispersion to individual nanotubes and there are a lot of functional groups on the nanotube surface. Thus, thermal defunctionalization at the above-mentioned ex situ condition on TEM grids might provide a valuable general way for imaging these functionalized SWNTs under optimized conditions.

In summary, we have reported successful HR-TEM imaging of aminopolymer-functionalized SWNT specimens at the level of individual nanotubes or their thin bundles before and after ex situ thermal defunctionalization. The corresponding EELS results confirm that most of the materials “wrapping” the SWNTs, as seen in the HR-TEM images, are associated with the aminopolymers functionalizing the nanotubes. The mechanistic details on the apparently strong interactions between SWNTs and the aminopolymers (i.e., the partition of covalent linkage, ionic interaction, or adsorption) remain to be understood, despite the fact that our functionalization reactions via



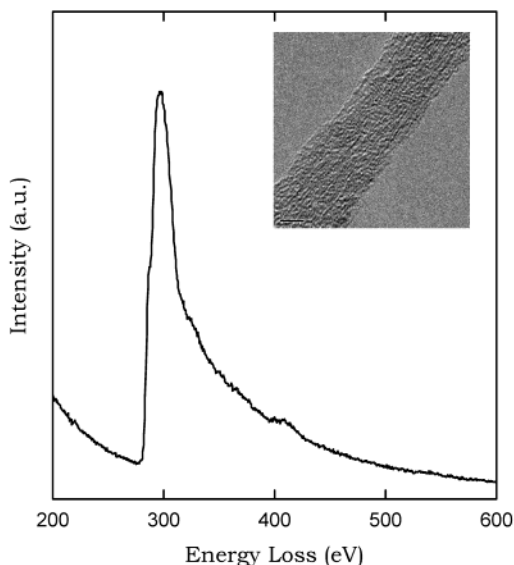


**Figure 9.** Typical EELS spectrum of a thin bundle of PPEI-EI-functionalized SWNT after ex situ thermal treatment, with the corresponding TEM image shown in the inset (scale bar = 5 nm).

diimide coupling target specifically the formation of covalent amide linkages. Further investigations by using both microscopic and bulk characterization (such as  $^{13}\text{C}$  NMR) techniques are required. Nevertheless, a combination of HR-TEM and EELS serves as a powerful tool for direct visual information of various functionalized nanotubes at the individual nanotube or thin bundle level, especially those containing heteroatoms.

**Acknowledgment.** We thank Prof. A. M. Rao and his students for providing the SWNT sample. Y.-P.S. acknowledges NSF, NASA, the South Carolina Space Grant Consortium, and the Center for Advanced Engineering Fibers and Films (NSF-ERC at Clemson University) for financial support. Research at Oak Ridge National Laboratory was sponsored by the Assistant Secretary for Energy Efficiency and Renewable Energy, Office of Transportation Technologies, as part of the High Temperature Materials Laboratory User Program, managed by UT-Battelle LLC for the U.S. Department of Energy under contract number DE-AC05-00OR22725.

## References and Notes

- (1) Niyogi, S.; Hamon, M. A.; Hu, H.; Zhao, B.; Bhowmik, P.; Sen, R.; Itkis, M. E.; Haddon, R. C. *Acc. Chem. Res.* **2002**, *35*, 1105.
- (2) Sun, Y.-P.; Fu, K.; Lin, Y.; Huang, W. *Acc. Chem. Res.* **2002**, *35*, 1096.
- (3) (a) Khabashesku, V. N.; Billups, W. E.; Margrave, J. L. *Acc. Chem. Res.* **2002**, *35*, 1087. (b) Hirsch, A. *Angew. Chem., Int. Ed.* **2002**, *41*, 1853. (c) Bahr, J. L.; Tour, J. M. *J. Mater. Chem.* **2002**, *12*, 1952.
- (4) Chen, J.; Hamon, M. A.; Hu, H.; Chen, Y.; Rao, A. M.; Eklund, P. C.; Haddon, R. C. *Science* **1998**, *282*, 95.
- (5) Chen, J.; Rao, A. M.; Lyuksyutov, S.; Itkis, M. E.; Hamon, M. A.; Hu, H.; Cohn, R. W.; Eklund, P. C.; Colbert, D. T.; Smalley, R. E.; Haddon, R. C. *J. Phys. Chem. B* **2001**, *105*, 2525.
- (6) Riggs, J. E.; Guo, Z.; Carroll, D. L.; Sun, Y.-P. *J. Am. Chem. Soc.* **2000**, *122*, 5879.
- (7) (a) Sun, Y.-P.; Huang, W.; Lin, Y.; Fu, K.; Kitaygorodskiy, A.; Riddle, L. A.; Yu, Y. J.; Carroll, D. L. *Chem. Mater.* **2001**, *13*, 2826. (b) Fu, K.; Huang, W.; Lin, Y.; Riddle, L. A.; Carroll, D. L.; Sun, Y.-P. *Nano Lett.* **2001**, *1*, 439.
- (8) Banerjee, S.; Wong, S. S. *J. Am. Chem. Soc.* **2002**, *124*, 8940.
- (9) Tang, B. Z.; Xu, H. *Macromolecules* **1999**, *32*, 5169.
- (10) Chen, J.; Liu, H.; Weimer, W. A.; Halls, M. D.; Waldeck, D. H.; Walker, G. C. *J. Am. Chem. Soc.* **2002**, *124*, 9034.
- (11) Czerw, R.; Guo, Z.; Ajayan, P. M.; Sun, Y.-P.; Carroll, D. L. *Nano Lett.* **2001**, *1*, 423.
- (12) Golberg, D.; Bando, Y.; Bourgeois, L.; Kurashima, K. *Carbon* **1999**, *37*, 1858.
- (13) Golberg, D.; Bando, Y.; Bourgeois, L.; Kurashima, K.; Sato, T. *Carbon* **2000**, *38*, 2017.
- (14) Suenaga, K.; Tence, T.; Mory, C.; Colliex, C.; Kato, H.; Okazaki, T.; Shinohara, H.; Hirahara, K.; Bandow, S.; Iijima, S. *Science* **2000**, *290*, 2280.
- (15) Hayashi, T.; Terrones, M.; Scheu, C.; Kim, Y. A.; Ruhle, M.; Nakajima, T.; Endo, M. *Nano Lett.* **2002**, *2*, 491.
- (16) Huang, W.; Lin, Y.; Taylor, S.; Gaillard, J.; Rao, A. M.; Sun, Y.-P. *Nano Lett.* **2002**, *2*, 231.
- (17) (a) Mawhinney, D. B.; Naumenko, V.; Kuznetsova, A.; Yates, J. T.; Liu, J.; Smalley, R. E. *Chem. Phys. Lett.* **2000**, *324*, 213. (b) Hamon, M. A.; Hu, H.; Bhowmik, P.; Niyogi, S.; Zhao, B.; Itkis, M. E.; Haddon, R. C. *Chem. Phys. Lett.* **2001**, *347*, 8.
- (18) A similar phenomenon has been reported by others on surface-modified MWNTs. See, for example: Shaffer, M. S. P.; Fan, X.; Windle, A. H. *Carbon* **1998**, *36*, 1603.
- (19) This image was from a sample deposited on a holey  $\text{LaCrO}_3$ -coated stainless steel grid, on which usually was found less surface tension effect than on holey carbon-coated copper grids.
- (20) The energy range of C-K EELS core loss is 268–370 eV for graphite and 266–368 eV for diamond. See online EELS and X-ray spectrum database at <http://www.cemes.fr/eelsdb>.